

Water nanodomain for efficient photocatalytic

CO₂ reduction to CO

Gang Chen^{a,b}, Xiuyan Cheng^{a,b}, Jianling Zhang^{*a,b}, Qiang Wan^{a,b}, Ran Duan^c, Buxing Han^{a,b}, Jie Cui^d, Junfeng Xiang^{b,d}, Bo Guan^d, Xueqing Xing^e, Guang Mo^e, Zhonghua Wu^e

^a Beijing National Laboratory for Molecular Sciences, CAS Key Laboratory of Colloid, Interface and Chemical Thermodynamics, CAS Research/Education Center for Excellence in Molecular Sciences, Institute of Chemistry, Chinese Academy of Sciences, Beijing 100190, P.R.China.

^b School of Chemical Science, University of Chinese Academy of Sciences, Beijing 100049, P.R.China.

^c CAS Key Laboratory of Photochemistry, Institute of Chemistry, Chinese Academy of Sciences Beijing 100190, P. R. China.

^d Center for Physicochemical Analysis and Measurement, Institute of Chemistry, Chinese Academy of Sciences Beijing 100190, P. R. China.

^e Beijing Synchrotron Radiation Facility (BSRF), Institute of High Energy Physics, Chinese Academy of Sciences, Beijing 100049, P.R.China.

*Corresponding authors:

E-mail addresses: zhangjl@iccas.ac.cn

Table of contents

- 1. Fig. S1** Droplet size distribution of water-in-oil microemulsion ($W_0=30$).
- 2. Fig. S2** Maximum absorption wavelength changes with W_0 of water-in-oil microemulsions.
- 3. Fig. S3** FT-IR spectra of $\text{Fe}(\text{tmhd})_3/n$ -hexane solution and microemulsions with $W_0=10, 30$ and 40 in wavenumber range of $400\text{-}4000\text{ cm}^{-1}$ (a) and $3100\text{-}4000\text{ cm}^{-1}$ (b).
- 4. Fig. S4** GC spectrum of gaseous mixture of the photocatalytic reaction.

Retention time: 3.345 min (Air), 3.849 min (CO) and 7.265 min (CO_2).
- 5. Fig. S5** Mass spectrometry signal and GC spectrum of the CO_2 reduction product using $^{13}\text{CO}_2$ as the feedstock.
- 6. Fig. S6** ^1H NMR spectra of water-in-oil microemulsion ($W_0=30$) at different temperatures.
- 7. Fig. S7** ^1H NMR spectra of the water-in-oil microemulsions with different W_0 values.
- 8. Fig. S8** UV-Vis spectra of $\text{Fe}(\text{tmhd})_3$ in n -hexane.
- 9. Fig. S9** Reaction mixture before (left) and after (right) reaction for 12 h.
- 10. Fig. S10** Molecular structures of $\text{Co}(\text{tmhd})_3$, $\text{Fe}(\text{acac})_3$, $\text{Fe}(\text{cp})_2$ and FeCl_3 .
- 11. Table S1** Control experiments of photocatalytic CO_2RR to CO.
- 12. Table S2** Performances of the reported photocatalytic CO_2RR to CO and this work.

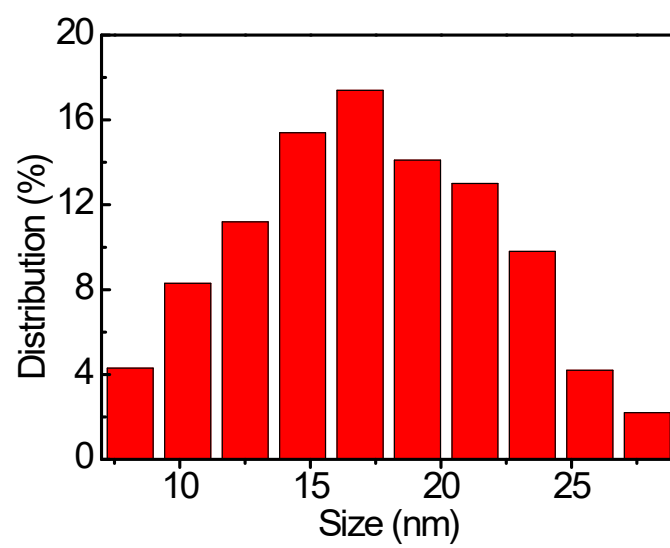


Fig. S1 Droplet size distribution of water-in-oil microemulsion ($W_0=30$).

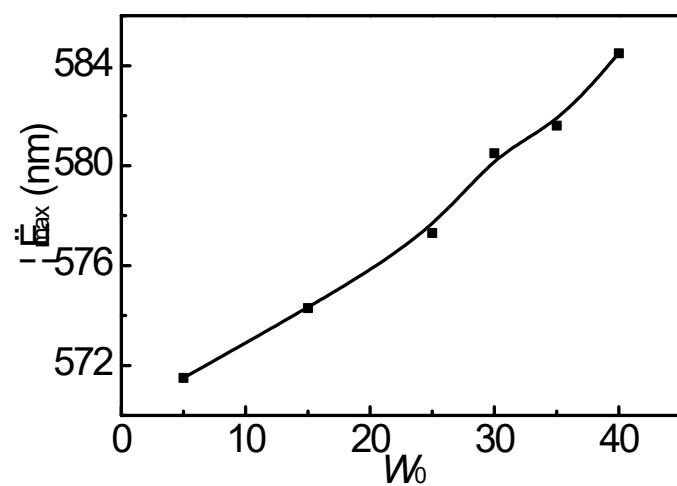


Fig. S2 Maximum absorption wavelength changes with W_0 of water-in-oil microemulsions.

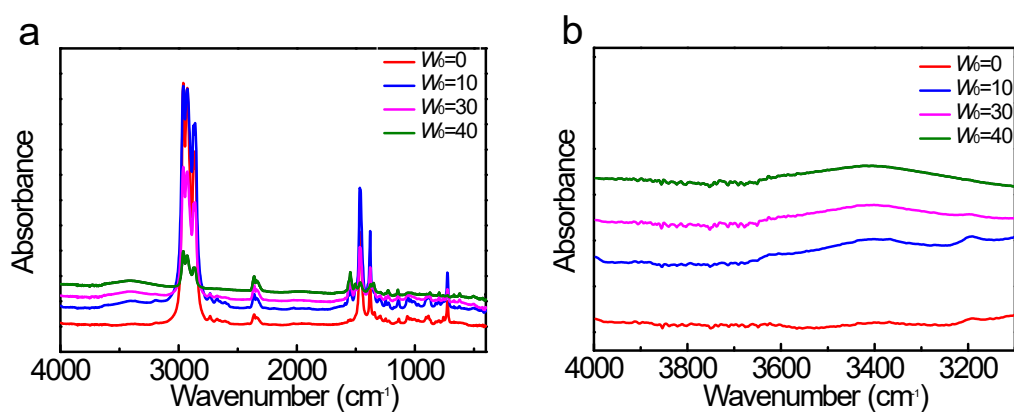


Fig. S3 FT-IR spectra of $\text{Fe}(\text{tmhd})_3/n$ -hexane solution and microemulsions with $W_0=10$, 30 and 40 in wavenumber range of 400-4000 cm^{-1} (a) and 3100-4000 cm^{-1} (b).

In $\text{Fe}(\text{tmhd})_3/n$ -hexane binary system, the absorptions at 2955, 2927 and 2858 cm^{-1} correspond to the stretching vibration of C-H. The absorptions at 1466 and 1385 cm^{-1} can be assigned to the bending vibration of C-H. For the water-in-oil microemulsion, the absorptions around 3200-3500 cm^{-1} appear and become stronger with increasing W_0 , indicating that more and more water molecules are dissolved in $\text{Fe}(\text{tmhd})_3/n$ -hexane system to form microemulsion.

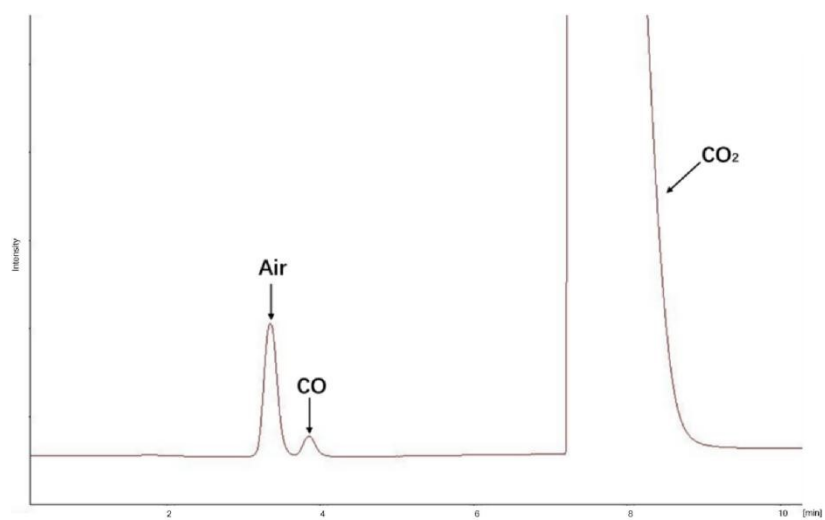


Fig. S4 GC spectrum of gaseous mixture of the photocatalytic reaction.

Retention time: 3.345 min (Air), 3.849 min (CO) and 7.265 min (CO₂).

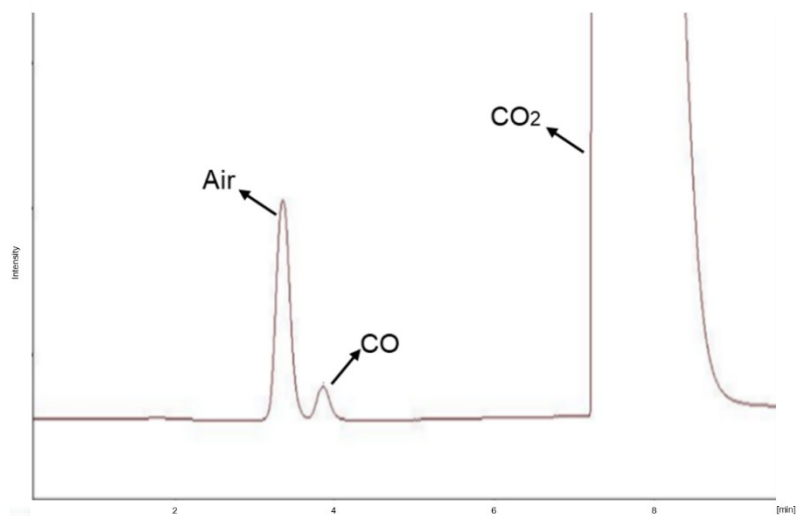
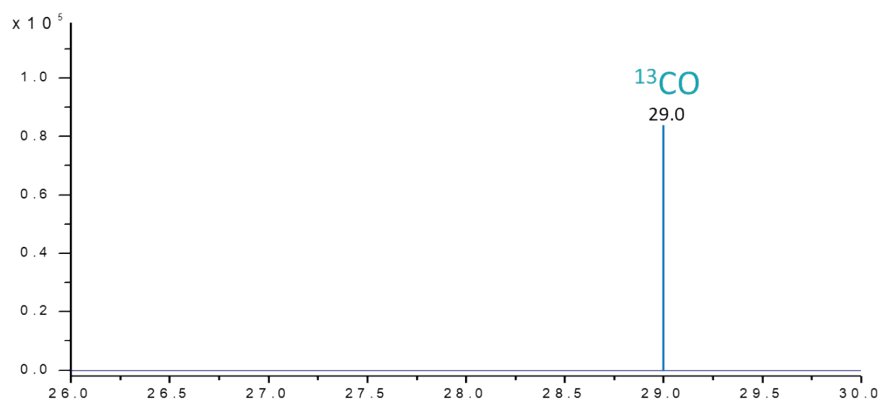


Fig. S5 Mass spectrometry signal and GC spectrum of the CO₂ reduction product using ¹³CO₂ as the feedstock.

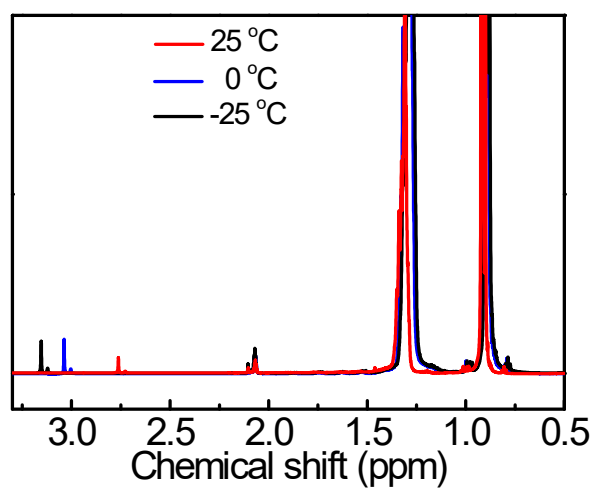


Fig. S6 ¹H NMR spectra of water-in-oil microemulsion ($W_0=30$) at different temperatures.

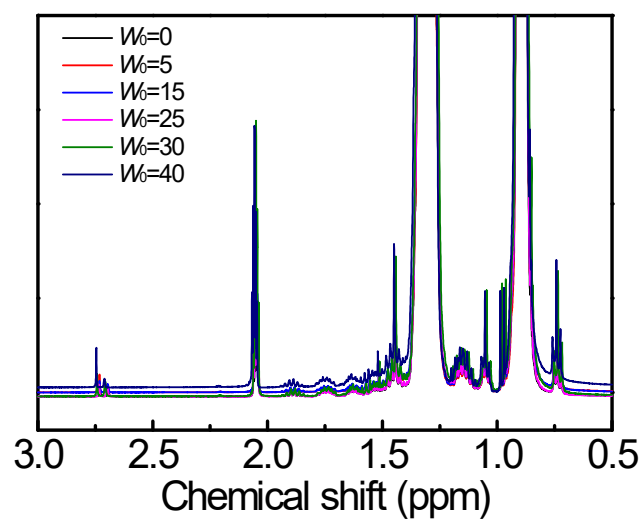


Fig. S7 ¹H NMR spectra of the water-in-oil microemulsions with different W_0 values.

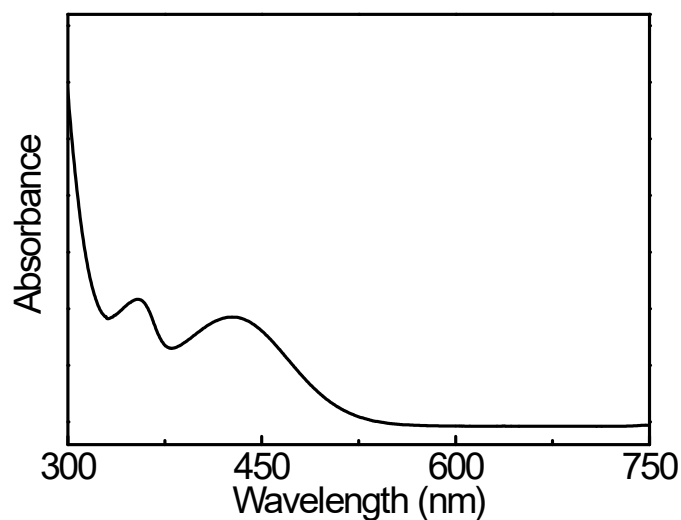


Fig. S8 UV-Vis spectrum of Fe(tmhd)₃ in *n*-hexane.

The absorption with λ_{max} of 356 nm is caused by charge transition and belongs to M→L transition. The valence electron layer of the central ion Fe³⁺ is configured with d⁵ electrons, and its anti-orbital π^* orbital is filled with 5 electrons, which can only accept electrons from the ligand π -orbital transition, and excess electrons can transit to the π orbital of ligand. The absorption with λ_{max} of 428 nm is caused by the transition of the conjugated π electron in the ligand tmhd⁻ and belongs to $\pi \rightarrow \pi^*$ transition.



Fig. S9 Reaction mixture before (left) and after reaction for 12 h (right).

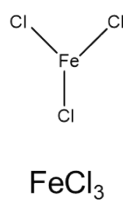
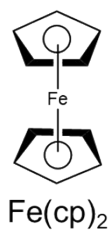
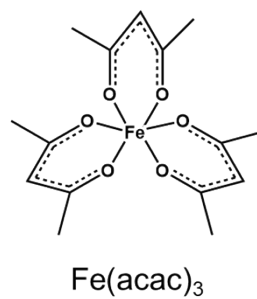
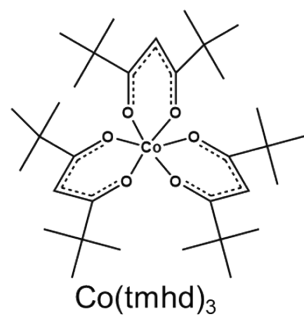


Fig. S10 Molecular structures of Co(tmhd)₃, Fe(acac)₃, Fe(cp)₂ and FeCl₃.

Table S1 Control experiments of photocatalytic CO₂RR to CO.

Control Conditions	CO evolution rate ($\mu\text{mol g}^{-1} \text{h}^{-1}$)	Selectivity (%)
Normal ^[a]	682	> 99%
No CO ₂	0	0
No Fe(tmhd) ₃	0	0
No light	0	0

^[a]Reactions conditions: 6.0 mg of Fe(tmhd)₃, 8.0 mL of *n*-hexane, CO₂ 0.1 MPa, $W_0=30$, 300 W Xe lamp, wavelength > 360 nm, reaction time 12 h.

Table S2 Performances of the reported photocatalytic CO₂RR to CO and this work.^[a]

Catalysts	Solvent	Light	CO evolution rate ($\mu\text{mol g}^{-1} \text{h}^{-1}$)	Selectivity (%)	Ref.
Co-ZIF-9/TiO ₂	H ₂ O	>200 nm	17.58	90.0	1
CPO-27-Mg/TiO ₂	H ₂ O	~365 nm	4.09	63.5	2
ZnIn ₂ S ₄	H ₂ O	400 nm	33.2	-	3
BiOBr atomic layers	H ₂ O	visible light	87.4	-	4
Bi ₁₂ O ₁₇ C ₁₂ nanotubes	H ₂ O	300 W Xe lamp	48.6	-	5
HKUST-1/Cu ₂ O/TiO ₂	H ₂ O	>320 nm	85	35.4	6
ZIF-67/CsPbBr ₃	H ₂ O	>420 nm	29.6	24.2	7
MOF-74-Mg/Zn ₂ GeO ₄	MeCN/H ₂ O (v:v=4:1)	>200 nm	12.94	100	8
NH ₂ -UiO-66/CsPbBr ₃	EtOAC/H ₂ O (v:v=300:1)	>420 nm	8.21	97.0	9
Eosin Y-functionalized COP	H ₂ O	>420 nm	33	92	10
porphyrin-tetra thiafulvalene COF-Zn	H ₂ O	420-800	~20	100	11
polymer-TiO ₂ -graphene composite	H ₂ O	>420 nm	~22	-	12
CT-COF	H ₂ O	>420 nm	102.7	98	13
Hypercrosslinked polymer	H ₂ O	UV-vis	~16	-	14
Fe(tmhd) ₃	<i>n</i> -hexane/H ₂ O (v:v=667:1)	>360 nm	682	>99	This work

^[a]For all these reactions, water was used as only sacrificial, involving no additional sacrificial donor.

REFERENCES

- [1] S. Yan, S. Ouyang, H. Xu, M. Zhao, X. Zhang and J. Ye, *J. Mater. Chem. A*, 2016, **14**, 15126-15133.
- [2] M. Wang, D. Wang and Z. Li, *Appl. Catal. B Environ.*, 2016, **183**, 47-52.
- [3] X. C. Jiao, Z. W. Chen, X. D. Li, Y. F. Sun, S. Gao, W. S. Yan, C. M. Wang, Q. Zhang, Y. Lin, Y. Luo and Y. Xie, *J. Am. Chem. Soc.*, 2017, **139**, 7586-7594.
- [4] J. Wu, X. D. Li, W. Shi, P. Q. Ling, Y. F. Sun, X. C. Jiao, S. Gao, L. Liang, J. Q. Xu, W. S. Yan, C. M. Wang and Y. Xie, *Angew. Chem. Int. Ed.*, 2018, **57**, 8719-8723.
- [5] J. Di, C. Zhu, M. Ji, M. Duan, R. Long, C. Yan, K. Gu, J. Xiong, Y. She, J. Xia, H. Li and Z. Liu, *Angew. Chem. Int. Ed.*, 2018, **57**, 14847-14851.
- [6] H. Zhao, X. Wang, J. Feng, Y. Chen, X. Yang, S. Gao and R. Cao, *Cat. Sci. Technol.*, 2018, **8**, 1288-1295.
- [7] X. He and W.-N. Wang, *J. Mater. Chem. A*, 2018, **6**, 932-940.
- [8] Z.-C. Kong, J.-F. Liao, Y.-J. Dong, Y.-F. Xu, H.-Y. Chen, D.-B. Kuang and C.-Y. Su, *ACS Energy Lett.*, 2018, **3**, 2656-2662.
- [9] S. Wan, M. Ou, Q. Zhong and X. Wang, *Chem. Eng. J.*, 2019, **358**, 1287-1295.
- [10] X. Yu, Z. Yang, B. Qiu, S. Guo, P. Yang, B. Yu, H. Zhang, Y. Zhao, X. Yang, B. Han and Z. Liu, *Angew. Chem. Int. Ed.*, 2019, **58**, 632-636.
- [11] M. Lu, J. Liu, Q. Li, M. Zhang, M. Liu, J.-L. Wang, D.-Q. Yuan and Y.-Q. Lan, *Angew. Chem. Int. Ed.*, 2019, **58**, 12392-12397.
- [12] S. Wang, M. Xu, T. Peng, C. Zhang, T. Li, I. Hussain, J. Wang and B. Tan, *Nat. Commun.*, 2019, **10**, 676.
- [13] K. Lei, D. Wang, L. Ye, M. Kou, Y. Deng, Z. Y. Ma, L. Wang and Y. Kong, *ChemSusChem*, 2020, **13**, 1725-1729.
- [14] G. E. M. Schukraft, R. T. Woodward, S. Kumar, M. Sachs, S. Eslava and C. Petit, *ChemSusChem*, 2021, **14**, 1-9.